Site Response and Model Uncertainty of Ground Motions in California

Tianqing Cao, Mark D. Petersen, Chris J. Wills, and Michael S. Reichle

Abstract

The release of the Next Generation Attenuation (NGA) relations affords an opportunity for comparing the predicted site responses and evaluating the ground motion model uncertainties due to site responses in seismic hazard analysis. From our preliminary comparisons, we found that the site amplifications of peak ground acceleration (PGA) and spectral acceleration (SA) at short periods predicted by the NGA relations are very close to the NEHRP (National Earthquake Hazard Reduction Program provisions, BSSC, 1994 and 1997) predictions. But for SA at one-second period, NEHRP predicts higher amplifications at low ground motion levels (< 0.2 g) and low amplifications at high ground motion levels (> 0.2 g) than the NGA relations. At one-second period, the NGA relations predict lower nonlinearity than NEHRP. These differences would have significant engineering implications. The NGA relations all use average shear wave velocities in the upper 30 m (V_{S30}) to estimate site amplifications. Two sources in site responses contribute to the ground motion model uncertainty: different formulations of site amplifications and the model uncertainty of shear wave velocity itself. We found that the ground motion uncertainty due to site responses predicted by NGA relations in California, which is measured by the coefficient of variation (COV, ratio of the standard deviation to the mean), is about 10% and fluctuates slightly for PGA on firm rock

(V_{S30} =760 m/s) with a 475-year return period. It almost does not depend on the ground motion levels and is uniformly distributed without any spatial pattern. Adding the uncertainty due to shear wave velocity uncertainties to the model uncertainty of the 2002 California hazard model, in which shear wave velocity uncertainty is not included, does not alter the spatial pattern of COV, which is closely related to the ground motion levels and fault distributions.

Introduction

Site response is an important factor to consider as it can contribute over a factor of two to different ground motions. In the widely used NEHRP site condition classification system six categories from classes A to F were defined using average shear wave velocities in the upper 30 m. The amplification factor for each soil class was given relative to class B. Recently, Wills and Clahan (2006) added many intermediate categories to the NEHRP categories for California and updated the preliminary site-conditions map developed by California Geological Survey (Wills et al., 2000). The new release of the NGA relations by Campbell and Bozorgnia (CB, 2006), Boore and Atkinson (BA, 2006), and Chiou and Youngs (CY, 2006) (the Pacific Earthquake Engineering Research Center, http://peer.berkeley.edu/NGA_program/) provides us an opportunity to compare the site amplification predictions between the NGA relations and the NEHRP.

A complete probabilistic treatment for the site amplification was formulated by Cramer (2005) as:

$$P(A_S > A_0 \mid M, R) = 1 - \int_{A_r} P(A_S \le A_0 \mid A_r) P(A_r \mid M, R) dA_r$$

where on the left side is the probability for ground motion A_S at a soil site greater than a given value A_0 for given magnitude M at distance R from the site; on the right side the integration is for all the possible ground motion A_r on a reference bedrock site for given M and R. The conditional probabilities $P(A_S \le A_0 \mid A_r)$ and $P(A_r \mid M, R)$ are needed for the method to work. In the NGA relations, the probability for the ground motion on any soil condition is given directly. We no longer have to use the formula above.

The release of NGA relations also provides us an opportunity to complete the model uncertainty study of Cao et al. (2005) by adding the uncertainties due to the shear wave velocity uncertainty. In the study of Cao et al. (2005), which is referred to as Cao et al. in the following for conciseness, the model uncertainties of the 2002 update of California seismic hazard maps were estimated using a Monte Carlo simulation method. The sources of model uncertainties considered in that study (see the California logic tree in Cao et al.) included the use of multiple attenuation and fault area-magnitude relations, epistemic magnitude and fault slip rate uncertainties, the multiple earthquake recurrence processes (characteristic and Gutenberg-Richter), and implicitly the uncertainty due to multiple site response formulations. One important source of uncertainty, the shear wave velocity uncertainty, was not included in that study because all the attenuation relations, except the Boore et al. (1997) attenuation, used in the 2002 California hazard model did not provide a consistent method for evaluating the site amplifications as a function of shear wave velocity.

The NGA relations use mean shear wave velocities in the upper 30 m (V_{S30}) and PGA (CB and BA) or SA (CY) on rock to evaluate the site amplifications, which are represented in the NGA formulations by separate terms. The three NGA site amplification formulations all include a linear and nonlinear term and base the nonlinear scaling on a ground-motion parameter. These are similar to the model developed by Choi and Stewart (2005). In the 2002 California hazard model, all the attenuation relations used were for generic rock. Therefore, the uncertainty due to multiple site amplification formulations was implicitly included as part of the model uncertainty. But this part of the uncertainty contribution cannot be separated from other uncertainties. For the NGA relations this part of the uncertainty can be evaluated independently. To estimate the ground motion uncertainties due to the shear wave velocity uncertainties in California, we use the results of Wills and Clahan (2006). In their study, the mean shear wave velocities and their uncertainties are provided for 19 geologically defined categories in California. It is obvious that the shear wave velocity uncertainties of Wills and Clahan (2006) are larger than those from direct measurements and using their results for a site with measurements could overestimate the uncertainty.

The ground motions (PGA or SA) on rock needed as input for evaluating the uncertainty due to site amplifications are from the model uncertainty study of the 2002 California hazard model using a Monte Carlo simulation method (Cao et al.) It should be emphasized here that the ground motion uncertainty contained in the input from Cao et al. is the model uncertainty of the 2002 California hazard model, which uses those attenuation relations published in 1997 without separate site response terms in the

formulations. They are for generic rock or soil. This study is not to use the NGA relations, which contain separate site response terms, to recalculate the model uncertainty. The recalculation with NGA relations will change to anther hazard model other than the 2002 model. This study only uses the site response terms of the NGA relations to add the missing uncertainty contributions due to the shear wave velocity uncertainties to the 2002 California model uncertainty of Cao et al. So the uncertainty maps from this study are still for the 2002 California hazard model not for a new model that uses the NGA relations.

In the following we introduce the site amplification formulations of NGA first, which is followed by the comparison of the site amplification predictions between the NGA relations and NEHRP. Then we estimate the ground motion uncertainties due to site responses and add the part due to shear velocity uncertainties to the model uncertainty of Cao et al. to get the total model uncertainty for the Los Angeles region and state of California. It is beyond the scope of this study to evaluate the ground motions and their model uncertainties to a new Califonia hazard model, which uses the NGA relations.

Site Response in the NGA Relations and the Comparison with NEHRP

It is necessary to quote the site amplification formulations from the three NGA relations so the results of this study can be explained. The BA equation for predicting ground motion Y is:

$$\ln Y = F_M(M) + F_D(r_{jb}, M) + F_S(V_{s30}, r_{jb}, M) \qquad (1)$$

where M and r_{jb} are the magnitude and distance of Joyner and Boore (Boore et al., 1997). The three terms on the right side of (1) are for the magnitude and distance scaling, and for the site amplification, respectively. The site amplification term is given by the following equation (BA, 2006):

$$F_S = F_{LIN} + F_{NL} \qquad (2)$$

where F_{LIN} and F_{NL} denote the linear and nonlinear terms, respectively. The linear term depends on the shear wave velocity V_{S30} and the reference velocity V_{ref} (=760 m/s):

$$F_{LIN} = b_{lin} \ln(V_{s30} / V_{ref})$$

where b_{lin} is the slope controlling the linear factor. When V_{S30} is equal to the reference velocity the linear term vanishes and if it is greater than the reference velocity the nonlinear term vanishes ($b_{nl} = 0$). The nonlinear site amplification factor is

for $pga4nl \le a_1$:

$$F_{NL} = b_{nl}(pga_low / 0.1) \qquad (3)$$

for $a_1 < pga4nl \le a_2$:

$$F_{NL} = b_{nl} \ln(pga4nl / 0.1) + c[\ln(pga4nl / a_1)]^2 + d[\ln(pga4nl / a_1)]^3 \qquad (4)$$

for $a_2 < pga4nl$:

$$F_{NL} = b_{nl} \ln(pga4nl / 0.1) \qquad (5)$$

where b_{nl} is the slope controlling the nonlinear factor. Constants a_1, pga_low, and a_2 are 0.03, 0.06, and 0.09 g respectively. The cubic polynomial with constant coefficients c and d in (4) is introduced to have continuous derivative of F_S at the transition from (3) to (5). According to BA, $pga4nl$ is given by the equation for $\ln Y$, but with

different coefficients for getting $Y = pga$. BA also emphasized that they need only give approximately correct pga values on rock-like sites.

The site amplification term in the CB relation is given by the following equations:

for $V_{S30} < k_1$:

$$f_{site} = c_{10} \ln(V_{S30} / k_1) + k_2 (\ln(A_{1100} + c(V_{S30} / k_1)^n) - \ln(A_{1100} + c)) \qquad (6)$$

for $V_{S30} \geq k_1$:

$$f_{site} = (c_{10} + k_2 n) \ln(V_{S30} / k_1) \qquad (7)$$

In equations (6) and (7), a non-linear site-response model developed by Walling and Abrahamson (2006) was used to constrain the functional form. A_{1100} is the PGA value on a rock site with $V_{S30} = 1100$ m/s. The symbols c and n are period-independent constants and c_{10}, k_1 and k_2 are all period dependent coefficients, where c_{10} is the only parameter from empirical fitting (CB).

The site amplification term in the CY relation is given by the following equation:

$$f_{site} = f_1 \ln(V_{S30} / 1130) + f_2 \exp(f_3 \times (V_{S30} - 360)) \ln((SA_{1130} + f_4) / f_4) \qquad (8)$$

where the coefficients f_1, f_2, f_3, and f_4 are dependent on the ground motion periods.

These three sets of site amplification formulas shear some commonalities. They all have linear and nonlinear terms. The linear terms only depend on the shear wave velocity and a reference velocity but not on the rock PGA or SA levels. The reference velocities for BA and CY are 760 and 1130 m/s respectively. For CB it is period dependent and is 865

m/s for PGA and SA at 0.01 sec. When the shear wave velocity is equal to the reference velocity, the linear term vanishes in each of these attenuation relations. The nonlinear terms all depend on the shear wave velocity and PGA (BA and CY) or SA (CY) on a reference rock. The reference rocks are defined slight differently. For CB and CY, they are defined as rocks with V_{S30} 1100 and 1130 m/s, respectively. For BA, the nonlinear term in equations (3) – (5) is not simply defined as a function of PGA on reference rock. It is indirectly defined by the calculated ground motion $pga4nl$ on rock, which is calculated using the same formula for PGA (equation (1)) but with a set of different coefficients. It depends, therefore, on the magnitude and distance of the source. This dependence on magnitude and distance makes it impossible to plot the site amplification, which is the ratio of ground motions for two different shear wave velocities, simply as a function of PGA on reference rock. In the following we explore the possibility of making such a simple plot possible when some approximations are applied.

First, we study the differences between $pga4nl$ and pga for different magnitudes and distances and then the consequences on predicted ground motions if we replace $pga4nl$ in equations (4) and (5) simply by pga on reference rock with V_{S30} 760 m/s. Figure 1 shows the difference between $pga4nl$ and pga (V_{S30} = 760 m/s) as a function of distance for three magnitudes 5, 6, and 7. For magnitude 6, the difference is very small at all distances or ground motion levels. For magnitude 5, the difference increases with increasing ground motion level. For magnitude 7, the difference increases with decreasing ground motion level. For $pga4nl < a_1$, the difference does not have any consequences on the predicted ground motions because in this case formula (3) is valid.

In order to explore the effect of using pga on reference rock to replace $pga4nl$ in equations (4) and (5) for the calculations, we compare (Fig. 2) the predicted ground motions for the case of magnitude 7 in Figure 1 because it has the largest differences between $pga4nl$ and pga among other magnitude cases in Figure 1.

Figure 2 shows that the ground motions from using pga on reference rock as $pga4nl$ (denoted as "approximate" in the figure) are almost the same as the accurate calculation at all ground motion levels or distances. The shear wave velocity used in Figure 2 is 360 m/s (C-D boundary in NEHRP categories), which is around the lower limit used in this study or the lower cutoff limit for the shear wave velocity distribution with mean V_{S30} =760 m/s in Wills and Clahan (2006). For shear wave velocities higher than this value we expect the differences are even smaller (see (4) and (5)) because $b_{nl} = 0$ for $V_{ref} < V_{S30}$ (see BA, 2006). So Figure 2 demonstrates that for BA it is a very good approximation to use pga on reference rock (V_{S30} = 760 m/s) to replace $pga4nl$ for the ground motion uncertainty estimation. With this approximation, we can use the PGA output from the 2002 California hazard model directly to evaluate the uncertainty due to the site amplifications formulated in the three NGA relations without recalculating the ground motions on reference rock, which is needed if $pga4nl$ is used. With this approximation, we can extend the model uncertainty estimation of the 2002 update of the California hazard model (Cao et al.) to include the uncertainties due to site responses without changing the hazard model (change the attenuation relations used). With this

approximation, it also becomes possible to plot the site amplification as a function of PGA on rock for a chosen shear wave velocity.

The widely used NEHRP site amplification is defined to 6 site classes using also the top 30 m mean shear wave velocities. These classes are:

A Hard rock, (V_{S30} > 1500 m/s)

B Rock, (760 m/s < V_{S30} ≤ 1500 m/s)

C Very dense soil and soft rock (360 m/s < V_{S30} ≤ 760 m/s)

D Stiff soil, (180 m/s < V_{S30} ≤ 360 m/s)

E Soil, (V_{S30} < 180 m/s)

F Soils requiring site-specific evaluations.

The site amplification coefficients in NEHRP are all referring to class B (the coefficients for B at all ground motion levels equal to 1.0). But the shear wave velocity being referred for those SA values at the top of the NEHRP tables is for NEHRP BC or 760 m/s (Campbell, personal communication). So in the following the amplification factors are all referring to 760 m/s to ensure a fair comparison with the NEHRP coefficients. The NEHRP coefficients for short and one-second periods were derived from averaging the SA amplification factors (arithmetic average, Borcherdt, personal communication) in a range of periods. The coefficients for the short period (F_a, see table 4.1.2.4a in BSSC 1997) are from the average of 0.1 to 0.5 second and the coefficients for the one-second period (F_v, see table 4.1.2.4b in BSSC 1997) are from the average of 0.5 to 2.0 second. The coefficients for PGA are from table 1.4.2.3a (F_a, in BSSC 1994). But in the real

applications of the NEHRP coefficients a single period is usually used. We made two sets of plots, one following the same averaging of NEHRP for the NGA relations and the other using a single period for the NGA relations, to see how different they may be.

Figure 3 is the set of plots in which the NGA amplification factors for short and one-second periods (Fig. 3b and 3c) are from the averaging following NEHRP. For BA relation, the coefficients or 0.4 sec were not provided. We use log-log interpolation between 0.3 and 0.5 sec. Each site amplification factor before averaging is the ratio of PGA (Fig. 3a) or SA (Fig. 3b and 3c) for V_{S30} 360 m/s and 760 m/s. Because the CB and BA relations use PGA on rock to evaluate the site response (see formulas (1) to (7)) it is not possible to plot the SA amplification factor as a function of SA without applying relations to convert PGA to SA. It is also true that the CY relation needs the same conversion to plot the SA amplification as a function of PGA (see (8)). We used the relations from NEHRP, in which SA at short period is 2.5 times the PGA and SA at one-second period is equal to the PGA. These relations are used for making Fig. 3b and Fig. 3c respectively. Figure 3 shows that the amplification factors for the three NGA relations are very consistent to each other. The amplification factors increase with period slightly. For short period SA (Figs. 3b) the NEHRP amplification factor is very near the average amplification factor of the three NGA relations. For PGA (Fig.3a) the NEHRP amplification factor is slightly higher than the NGA factors at ground motion levels between 0.1 and 0.3g. For one-second period SA the NGA amplification factors almost overlap each other before 0.1g. But the NEHRP amplification factors are higher than the NGA factors at low ground motion levels (< 0.1g) and quickly decrease to lower than the

NGA factors at ground motion great than 0.3g. This quick decrease is the so-called high nonlinearity, which describes how the amplification factor changes with ground motion levels. Fig. 3c shows that the NEHRP nonlinearity for one-second period is higher than the NGA relations.

Figure 4 is the set of plots in which the NGA amplification factors are not from averaging over a period range but from single periods. We have chosen 0.2 and 1.0 sec for Figures 4a and 4b respectively so they are near the middle periods of the NEHRP averaging ranges for short and one-second periods respectively in Figures 3b and 3c. Figure 4 shows that they are not much different from the comparisons shown in Figures 3b and 3c. Comparing Figure 3b with Figure 4a and Figure 3c with Figure 4b we conclude that using NEHRP coefficients for single periods is acceptable as long as the period is near the middle of a NEHRP averaging range. For BA attenuation relation, the amplification factor for one-second period is a constant (Fig. 4b) or no nonlinearity. It is because for shear wave velocity greater than 300 m/s the nonlinear term F_{NL} vanishes. But in Figure 3c the averaging includes the SA amplification factor for 0.5 sec period and its nonlinear term is not zero, which causes a small slope for the BA curve.

Ground Motion Uncertainty due to Site Response

The ground motion uncertainties due to site response are from multiple site amplification formulations and shear wave velocity uncertainties. The inaccuracy of the soil maps is not considered here. The differences in site amplifications among the NGA relations

(Fig. 3) should determine if there are any characteristic uncertainty patterns related to ground motion levels or distances from the faults when all the NGA relations are used. In Cao et al., for example, the ground motion uncertainty (COV) due to attenuation relations was found to have a distance dependent pattern from faults. The uncertainty decreases from a fault to certain distance and then starts to increase. It reaches a minimum value at distances at around 30-50 km because of the larger data set for developing those attenuation relations in that distance range. We wish to find if the differences in site amplifications among the three NGA relations are ground motion level dependent. Because the CY and BA relations are so similar (Fig. 3a) for PGA we only check the differences between CY and CB relations to see if there are any characteristic patterns.

Figure 5 is the predicted PGA (V_{S30} =760 m/s) difference between CY and CB normalized by the PGA on reference rock (V_{S30} =1130 m/s) for CY. We made sure that the input PGA on CB reference rock produces ground motion on 1130 m/s rock always equal to the CY reference rock ground motion, which means that the slight difference on reference rock (1100 m/s vs. 1130 m/s) has been accounted. Figure 5 shows that for PGA up to about 0.4g the difference is almost a constant, which is only about 6%. The difference increases to about 8% when PGA increases to 0.8g. So we may expect the ground motion uncertainty (COV) due to site amplifications of the three NGA relations to fluctuate slightly without a characteristic spatial pattern related to the fault or ground motion distributions (see figures in the next section). That the differences do not change much with ground motion level is equivalent to not changing with distance from faults.

This independence to the ground motion levels is due to the functional similarities of the site amplification factors shown in Figure 3 for the three NGA relations. Because of this similarity, the epistemic uncertainty due to site amplification only may be slightly underestimated if only three NGA relations are used (personal communication, Campbell).

The uncertainty of shear wave velocity also contributes to the ground motion uncertainty through site amplifications. In Wills and Clahan (2006), the available shear wave velocity data (V_{S30}) in California were sorted by the generalized geological unit. The extent of the geologic map units then can be used to transfer the velocity characteristics from the sites where the velocities were measured to sites on the same or similar materials. This is a process to model the site conditions according to their similarities in geology and shear wave velocity. For a particular unit, the sorted shear wave velocities usually follow a lognormal distribution. These sorted velocities of a distribution are not from the same site but different measurements in the same soil category. So the scatter of the velocities is not the aleatory uncertainty of the shear wave velocity for the site, it is the epistemic uncertainty for the site. It is the epistemic uncertainty of shear wave velocity for the site (the standard error of the mean). It is related to how the geological units are defined or how the soils and rocks are grouped into those units. About 25-33% of the shear wave velocity data used to develop the NGA relations are measured with much smaller uncertainties than those from a geological approach of Wills and Clahan (2006). For those sites, our estimates of ground motion uncertainties are on the conservative side.

We have shown in Figure 5 that the normalized PGA differences between the three NGA relations remain constant until very high ground motion levels and cause the ground motion uncertainty (COV) to be similar for different risk (ground motion) levels. When this feature is applied to evaluate ground motion uncertainties for a uniform site condition, for example 760 m/s, but with shear wave velocity uncertainties (epistemic), we expect the uncertainty to fluctuate without a characteristic spatial pattern too. It is because the same epistemic velocity uncertainty is applied everywhere. The nonlinear terms for site amplifications, which depend on the ground motion levels, are much smaller than the linear terms, which do not depend on ground motion levels. For example, in formula (2) the linear term dominates over the nonlinear term for the shear wave velocity range relevant to this study ($V_{S30} \geq 300$ m/s) and for the ground motion levels of the 2002 California PGA map with a 475-year return period. The ground motions on this map are mostly in the range of 0.1 to 0.4g and exceed 0.4g at a few localized locations near active faults (Cao et al.).

Uncertainty Maps

Two types of ground motion uncertainty maps are presented here. One is for the sensitivity study to show the ground motion uncertainty (COV) due to each source of uncertainty. The other type is for the total uncertainty, which includes the model uncertainties studied by Cao et al. and the uncertainties due to shear wave velocity uncertainties. For the first type, we now have two additional sources other than those studied by Cao et al., different site amplification formulations of the NGA relations and

uncertainties of the shear wave velocities. Because of the NGA formulations, in which the site responses are represented by separate terms, we can evaluate the uncertainty contributions due to multiple site response formulations and shear wave velocity uncertainties separately. The input ground motions for producing a ground motion uncertainty map, which accounts for the site response formulations only, are the PGA values for a 475-year return period and V_{S30} 760 m/s from the 2002 California hazard model. These ground motions are used in a randomly selected NGA site amplification formula from three NGA relations to calculate the ground motions for a specific shear wave velocity (760 m/s). Therefore, the uncertainty (COV) is from the ground motion differences using different NGA site response terms for the same shear wave velocity. To produce a ground motion uncertainty map with multiple site response formulations and shear wave velocity uncertainties together, the input ground motions are still the PGA values for a 475-year return period and V_{S30} 760 m/s from the 2002 California hazard model. But the shear wave velocities used in those site response terms are also randomly selected from a lognormal distribution of Wills and Clahan (2006) for a given mean shear wave velocity that distribution describes the standard error of the mean shear wave velocity.

The other type of ground motion uncertainty map accounts for the total uncertainties of shear wave velocity uncertainties and other model uncertainties studied by Cao et al., which include the use of multiple attenuation relations (not NGA relations) and area-magnitude relations, epistemic magnitude and fault slip rate uncertainties, and the multiple earthquake recurrence processes (characteristic and Gutenberg-Richter). As we

have stated that because of the use of multiple attenuation relations for the same generic rock in the 2002 California hazard model, the uncertainty contribution equivalent to the multiple site response formulations has been implicitly included in the model uncertainties of Cao et al. In order to include the uncertainties studies by Cao et al., the PGA output from the Monte Carlo simulations of Cao et al., in which 150 iterations were performed for each simulation, is used as input. Three site amplification formulas of NGA are used with equal weights for a randomly selected shear wave velocity from the lognormal distribution (Wills and Clahan, 2006) for evaluating the total ground motion uncertainty. To average the ground motions from three NGA site amplification formulas for a selected shear wave velocity is to avoid double counting the uncertainties due to multiple site response formulations.

The maps for sensitivity studies are made for Los Angeles region only as we did in Cao et al. The maps for total uncertainty are made for the Los Angeles region and state of California. The ground motion model uncertainty maps that follow are all COV maps for PGA of the 2002 California hazard model with a 475-year return period on uniform soil conditions (NEHRP BC boundary or 760 m/s). Figure 6 shows the PGA uncertainty due to site amplification formulations only and is calculated using the PGA of 2002 California hazard model in the Los Angeles region as input. A Monte Carlo simulation is performed to randomly select one of the three NGA relations for calculating the site amplifications with V_{S30} =760 m/s (no shear wave velocity uncertainties). As expected the uncertainty is low and fluctuates around 6-7% without any spatial pattern related to faults or ground motion levels. This level of uncertainty is the lowest compared with

uncertainties from other sources as shown in the sensitivity analysis of Cao et al. (Fig. 12) for the Los Angeles region. It happens to be similar to the uncertainty level of the background seismicity source.

The second part of the uncertainty related to site response is due to the shear wave velocity uncertainty itself. In Wills and Clahan (2006), the geologic units for shear wave velocity near 760 m/s are Franciscan complex rock (KJF) and crystalline rocks (xtaline) (see their Table 1). The mean V_{S30} for these units are 782 and 748 m/s, respectively. We use the average mean of $\ln(V_{S30})$ and its standard deviation to evaluate the ground motion uncertainty due to the uncertainty of V_{S30}. Figure 7 is the uncertainty map for shear wave velocity uncertainty only. It is the V_{S30} uncertainties with a mean value of 760 m/s. It is slightly higher than the uncertainty due to multiple site response formulation in Figure 6. Because V_{S30} is used in the linear amplification terms and these terms dominate the amplifications but do not depend on the PGA levels, the ground motion uncertainty due to V_{S30} uncertainty also does not have any characteristic spatial patterns related to ground motion levels or fault distributions. So the uncertainty of the amplification formulations and the V_{S30} uncertainty together should also have a uniform spatial distribution with small fluctuations. The two sources from site response together (Figs. 6 and 7) will contribute uncertainties (COV) around 10%.

Figure 8 is the ground motion uncertainty map that includes all the uncertainties studied in Cao et al. and the uncertainty due to shear wave velocity uncertainty in this study. The

input ground motions for evaluating the uncertainties in Figure 8 are the PGA from 150 Monte Carlo simulations of Cao et al., which are from sampling the California logic tree and contain the ground motion model uncertainties other than the uncertainty due to shear wave velocity uncertainty. To include the uncertainties of shear wave velocity, we randomly select a shear wave velocity from the lognormal distribution of Wills and Clahan (2006) for mean V_{S30} = 760 m/s and use this velocity in all three NGA relations and then average the output with equal weights. The average process is not to double count the uncertainties due to multiple site response formulations. To compare Figure 8 with the COV map of Cao et al. (2005, Fig. 11), we find that the COV values are increased by a few percent because the added uncertainties due to the shear wave velocity uncertainty.

Figure 9 is the total model uncertainty map for California for PGA on firm rock (BC boundary or V_{S30} =760 m/s) with a 475-year return period. It is produced like Figure 8 to include the ground motion model uncertainties of the 2002 California hazard model (Cao et al.) and the uncertainties due to shear wave velocity. In general the COV is increased by a few percent in comparing with Figure 16 of Cao et al. because the added uncertainties due to shear wave velocity uncertainty. Since the independent uncertainties are added up as the square root of the sum of the squares of each uncertainty, we see more significant increases at originally low COV regions such as the great valley region in central California, where the COV value increased from 5-10% to 10-15%. Figure 9 also shows that adding the uncertainty due to shear wave velocity uncertainty does not

alter the general pattern of COV in California, which is dominated by the fault distribution.

Summary and Discussions

In this study, the site amplification factors predicted by the NGA relations and NEHRP are compared. We found that for PGA and short period SA both predictions agree with each other for a wide range of ground motion levels. For one-second SA NEHRP predicts higher amplifications than NGA relations for ground motion less than 0.3 g. For ground motion higher than 0.3 g NEHRP amplification factor decreases to lower than the NGA amplification factors, which means that the nonlinearity of the NEHRP amplification factor is higher than the NGA amplification factor at this period. This difference may have some important engineering implications. The ground motion uncertainties due to site responses, which are from the multiple site response formulations and shear wave velocity uncertainties, are low compared with other model uncertainties studied by Cao et al. for the 2002 California hazard model. The uncertainties due to site responses have a uniform spatial distribution and are independent to the fault distribution.

Normally, we expect the uncertainty due to multiple attenuation relations (not multiple site response terms only) to be distance dependent from the faults because the data constraint is always the best at certain distances around 30 to 50 km. The site amplification differences among the three NGA relations showed no such correlation to

the distance or equivalently to the ground motion levels. We attribute this to the similarity of the site amplification formulations and the consistency of the data sets used by the NGA developers. Another reason for the uniform distribution of the site response uncertainty is the domination of the linear term over the nonlinear term in the site response formulas. The linear term depends only on the shear wave velocity and not the PGA or SA levels on reference rock. So when an uncertainty distribution of shear wave velocity is called for a region with a uniform shear wave velocity, the uncertainty of ground motion is also spatially uniform. The nonlinear term, which depends on both the shear wave velocity and PGA or SA on rock, causes only small spatial fluctuations of the uncertainty.

We have extended the ground motion model uncertainties of the 2002 California hazard model (Cao et al.) to include the uncertainties due to shear wave velocity uncertainty. We found that the ground motion uncertainties of the 2002 California hazard model studied by Cao et al., which showed a strong spatial pattern following the fault distributions in California, are not altered by adding the shear wave velocity uncertainties. It is because the added uncertainty is lower compared with the other model uncertainties and the added uncertainty has a very uniform spatial distribution.

The NGA relations provide site response evaluations for any given shear wave velocities. It allows us to discuss some of the issues related to the use of old attenuation relations, which usually do not have a clear definition to what shear wave velocity they were refer to. The old attenuation relations are usually defined for generic rock or soil. Figure 10 is

designed to show what is the impact to a ground motion map if the shear wave velocity selected for the generic rock or soil is off by some amount. In this figure, we used only the CY relation. We see if the generic rock with V_{S30} = 520 m/s is used for a map for V_{S30} =760 m/s (NEHRP B-C boundary) without any corrections, the PGA in a hazard map will be over predicted by 20% at very low ground motion levels and gradually decreases to about 15% at 0.1g. For SA at 1 second, the over prediction is about 35% at low ground motion levels and decreases very little at higher levels. If the shear wave velocity 760 m/s for NEHRP B-C boundary is used as NEHRP B and assuming the central value 1130 m/s for B, the over predictions are about 22% and 37% for PGA and SA. This kind of over predictions may have happened for 2002 California hazard maps (Cao, et al.).

This study shows that the newly developed NGA attenuation relations not only enable a consistent ground motion estimation on any given soil types but also for the first time demonstrated that the model uncertainty due to site response is lower compared with other parts of the hazard model uncertainties provided the soil is well defined with its shear wave velocity. It is another confirmation to the approach of using shear wave velocity and the input reference rock motion to model the nonlinear site amplifications.

Acknowledgements

This study is supported by USGS/HEHRP grant 05HQGR0030. The authors are grateful to Kenneth Campbell, Roger Borcherdt, Norm Abrahamson, and David Boore for many helpful discussions and suggestions.

References

Boore, D. M., W. B. Joyner, and T. E. Fumal (1997). Equations for estimating horizontal response spectra and peak acceleration from western North America earthquakes: a summary of recent work. *Seism. Res. Lett.* **68**, 128-153.

Boore, D. M., and G. M. Atkinson (2006). Boore-Atkinson provisional NGA empirical ground-motion model for the average horizontal component of PGA, PGV and SA at spectral periods of 0.05, 0.1, 0.2, 0.3, 0.5, 1, 2, 3, 4, and 5 seconds.

BSSC (1994). NEHRP recommended provisions for seismic regulations for new buildings, Part 1-Provisions, FEMA 222A, Federal Emergency Management Agency, 290pp.

BSSC (1997). NEHRP recommended provisions for seismic regulations for new buildings, Part 1-Provisions, FEMA 302, Federal Emergency Management Agency, 337pp.

Campbell, K., and Y. Bozorgnia (2006). Campbell-Bozorgnia NGA empirical Ground motion model for the average horizontal component of PGA, PGV, PGD, and SA at selected spectral periods ranging from 0.01-10.0 seconds.

Cao, T, M. D. Petersen, and A. D. Frankel (2005). Model uncertainties of the 2002 update of California seismic hazard maps, *Bull. Seism. Soc. Am.*, **95**, no. 6, 2040-2057.

Chiou, B., and R. Youngs (2006). Chiou and Youngs PEER-NGA empirical ground motion model for the average horizontal component of peak acceleration and pseudo-spectral acceleration for spectral periods of 0.01 to 10 seconds.

Choi, Y. and J. P. Stewart (2005). Nonlinear site amplification as function of 30 m shear wave velocity, *Earthquake Spectra*, **21**, no. 1, 1-30.

Cramer, C. H. (2005). Erratum: Site-Specific seismic-hazard analysis that is completely probabilistic, *Bull. Seism. Soc. Am.* **95**, no. 5, 2026.

Walling, M., and N. Abrahamson (2006). Non-linear soil response model. In Proceedings, Eighth National Conference on Earthquake Engineering, Paper No. 1030.

Wills, C. J., M. D. Petersen, W. A. Bryant, M. S. Reichle, G. J. Saucedo, S. S. Tan, G. C. Taylor, and J. A. Treiman (2000) A site conditions map for California based on geology and shear wave velocity, *Bull. Seism. Soc. Am.* **90**, no. 6b, S187-S208.

Wills, C. J., and K. B. Clahan (2006). Developing a map of geologically defined site-condition categories, *Bull. Seism. Soc. Am.* **96**, no. 4A, 1483-1501.

Authors

Tianqing Cao
California Geological Survey
801 K Street, MS 12-32
Sacramento, CA 95814

Mark D. Petersen
U. S. Geological Survey
Box 25046 Federal Center, MS 966
Denver, Colorado 80225

Chris J. Wills
California Geological Survey

801 K Street, MS 12-32
Sacramento, CA 95814

Michael S. Reichle
California Geological Survey
801 K Street, MS 12-32
Sacramento, CA 95814

Figure Captions

Figure 1: Comparison of PGA (V_{S30} =760 m/s) to $pga4nl$ in BA attenuation relation. The departure of the two ground motion values occurs at large distances for magnitude 7.0 and at short distances for magnitude 5.0.

Figure 2: Comparison of the PGA values between "accurate" and "approximate" calculations as a function of distance. The solid line (accurate) is for PGA calculated following formulas (3) – (5) exactly; the dash line (approximate) is for PGA calculated using PGA on rock (V_{S30} =760 m/s) to replace $pga4nl$ in formulas (4) and (5). For $pga4nl \le a_1 (= 0.03g)$, formula (3) is used and it does not contain $pga4nl$. So the two lines overlap with each other.

Figure 3: Comparison of NEHRP coefficients and NGA site amplification factors for (a) PGA, (b) short period SA, and (c) one-second SA. The amplification factor is the ground motion ratio between V_{S30} 360 and 760 m/s. The amplification factors for the NGA relations are the average from 0.1 to 0.5 sec for (b) and 0.5 to 2.0 sec for (c) following the same way to develop the NEHRP coefficients (open squares). For the BA curve, $pga4nl$ is approximated by pga for V_{S30} =760 m/s.

Figure 4: Comparison of NEHRP coefficients and NGA site amplification factors for (a) short period SA and (b) one-second period SA. The difference from Figures 3b and 3c are that the NGA amplification factors are from single periods near the middle points of the averaging ranges in Figure 3, which are 0.2 sec for (a) and 1 sec for (b).

Figure 5: The predicted PGA (V_{S30} =760 m/s) difference between CY and CB attenuation relations as a function of PGA (V_{S30} =1130 m/s) for CY. The difference is normalized by the PGA on rock (V_{S30} =1130 m/s). This curve shows that the difference between CY and CB is almost a constant until PGA greater than 0.3 to 0.4 g.

Figure 6: COV of PGA (475-year return period) map for the Los Angeles region for uncertainties from site amplification formulations only. The COV value fluctuates around 6% uniformly, which is similar to the value predicted in Figure 5. No spatial patterns related to faults or ground motion levels are observed. The thick line is the coastline.

Figure 7: COV of PGA (475-year return period) map for the Los Angeles region for uncertainties from the shear wave velocity uncertainty only. The COV value fluctuates around 7-8% uniformly. No Spatial patterns related to faults or ground motion levels are observed. The thick line is the coastline.

Figure 8: COV of PGA (475-year return period) map for the Los Angeles region for uncertainties from the shear wave velocity uncertainty and the epistemic model uncertainty of Cao et al., in which the uncertainty due to multiple site response formulations is implicitly included through random selection of the attenuation

relations. Because the ground motion uncertainty from shear wave velocity uncertainty is much lower than other epistemic model uncertainty and it is spatially uniform, the spatial pattern of the other epistemic model uncertainty is not altered by adding the uncertainty due to shear wave velocity. The COV value in the low COV region of the epistemic model uncertainty increases more noticeably. The thick line is the coastline.

Figure 9: COV of PGA (475-year return period) map for California. The mean shear wave velocity used is for firm rock or 760 m/s. It is for the total model uncertainty, which includes the model uncertainty of Cao et al. and the added uncertainty due to shear wave velocity.

Figure 10: The amplification factors for various shear wave velocities for the CY relation. It is to be used to show the percentage of over prediction of PGA and SA at 1 second if the shear wave velocity used is lower than the true value.

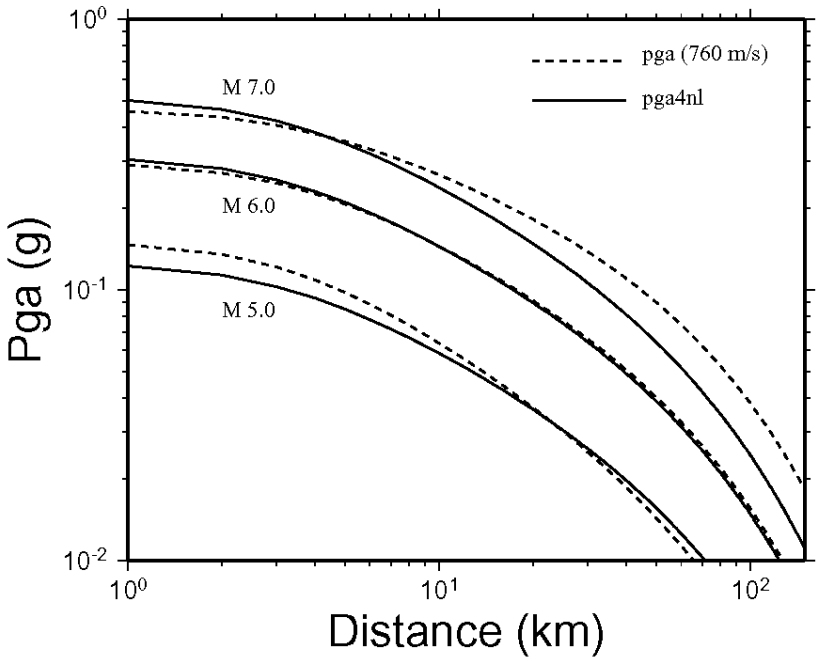
pga (760 m/s)
pga4nl
M 7.0
M 6.0
M 5.0
Pga (g)
Distance (km)
10^0
10^{-1}
10^{-2}
10^0
10^1
10^2

Fig. 1

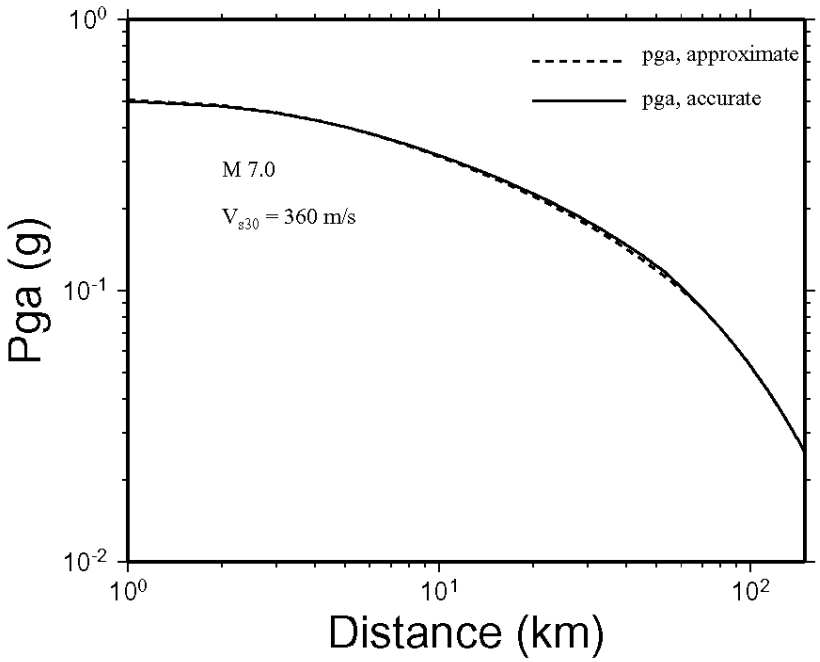
pga, approximate
pga, accurate
M 7.0
V_{s30} = 360 m/s
Pga (g)
Distance (km)
10^0
10^{-1}
10^{-2}
10^0
10^1
10^2

Fig. 2

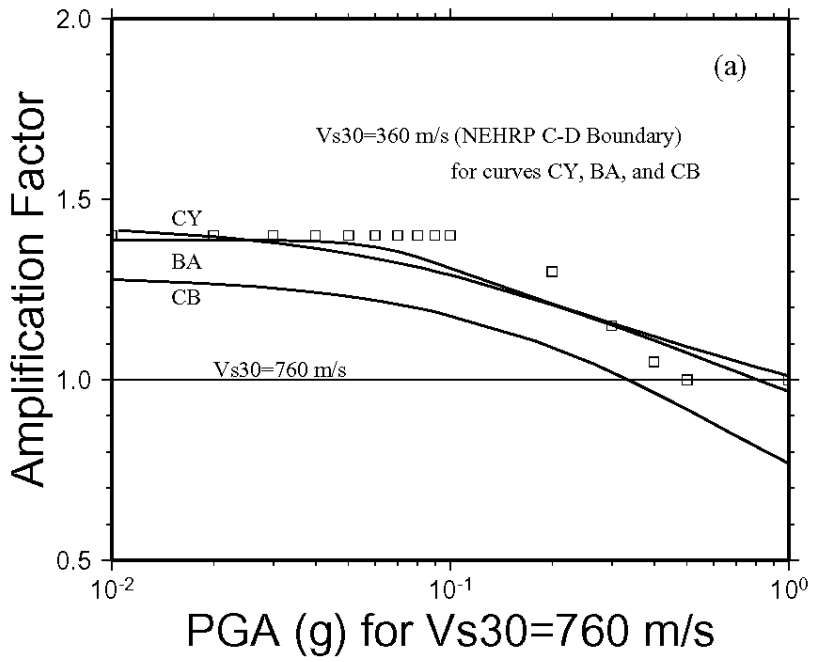
(a)
Vs30=360 m/s (NEHRP C-D Boundary)
for curves CY, BA, and CB
CY
BA
CB
Vs30=760 m/s
Amplification Factor
PGA (g) for Vs30=760 m/s
2.0
1.5
1.0
0.5
10^{-2}
10^{-1}
10^{0}

Fig. 3a

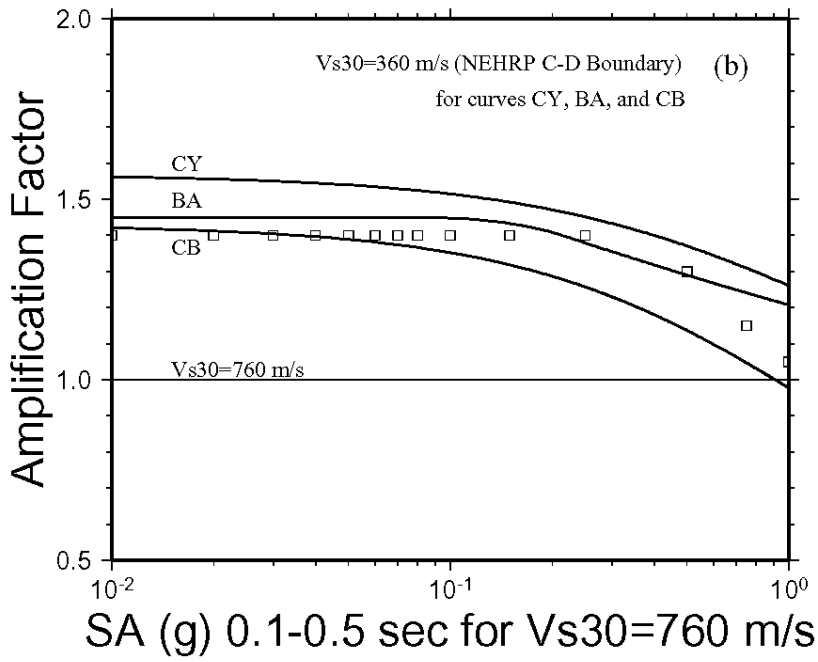
Vs30=360 m/s (NEHRP C-D Boundary)
for curves CY, BA, and CB
(b)
CY
BA
CB
Vs30=760 m/s
Amplification Factor
2.0
1.5
1.0
0.5
10^{-2}
10^{-1}
10^{0}
SA (g) 0.1-0.5 sec for Vs30=760 m/s

Fig. 3b

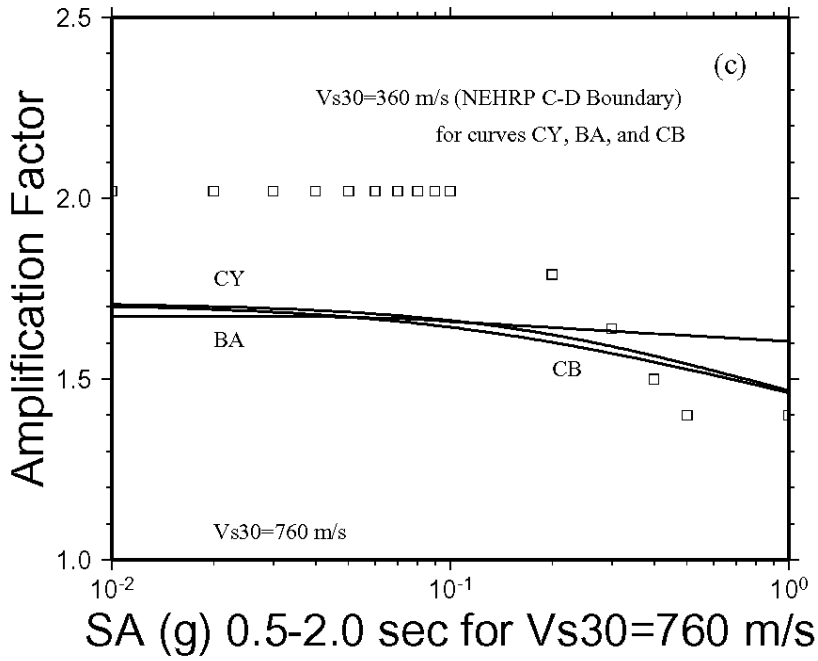
(c)
Vs30=360 m/s (NEHRP C-D Boundary)
for curves CY, BA, and CB
CY
BA
CB
Vs30=760 m/s
Amplification Factor
SA (g) 0.5-2.0 sec for Vs30=760 m/s
2.5
2.0
1.5
1.0
10-2
10-1
100

Fig. 3c

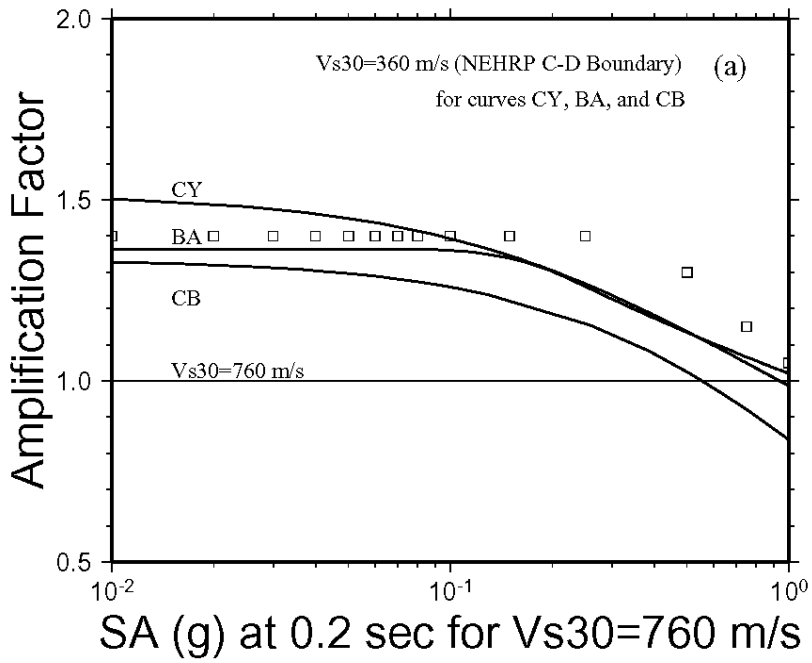
Vs30=360 m/s (NEHRP C-D Boundary)
for curves CY, BA, and CB
(a)
CY
BA
CB
Vs30=760 m/s
Amplification Factor
2.0
1.5
1.0
0.5
10^{-2}
10^{-1}
10^{0}
SA (g) at 0.2 sec for Vs30=760 m/s

Fig. 4a

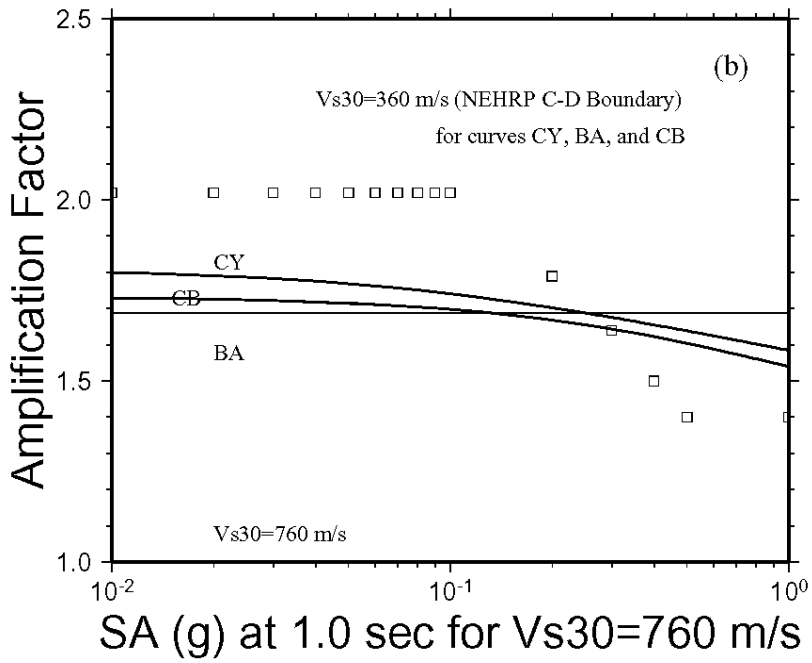
(b)
Vs30=360 m/s (NEHRP C-D Boundary)
for curves CY, BA, and CB
CY
CB
BA
Vs30=760 m/s
Amplification Factor
SA (g) at 1.0 sec for Vs30=760 m/s
2.5
2.0
1.5
1.0
10-2
10-1
100

Fig. 4b

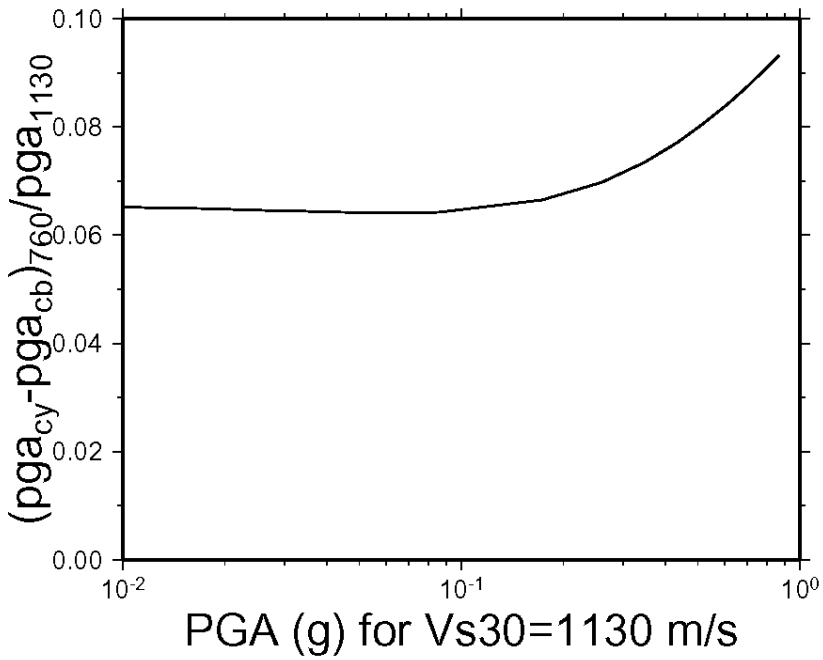
0.10
0.08
0.06
0.04
0.02
0.00
$(pga_{cy}-pga_{cb})_{760}/pga_{1130}$
10^{-2}
10^{-1}
10^{0}
PGA (g) for Vs30=1130 m/s

Fig. 5

Site Amplification Only

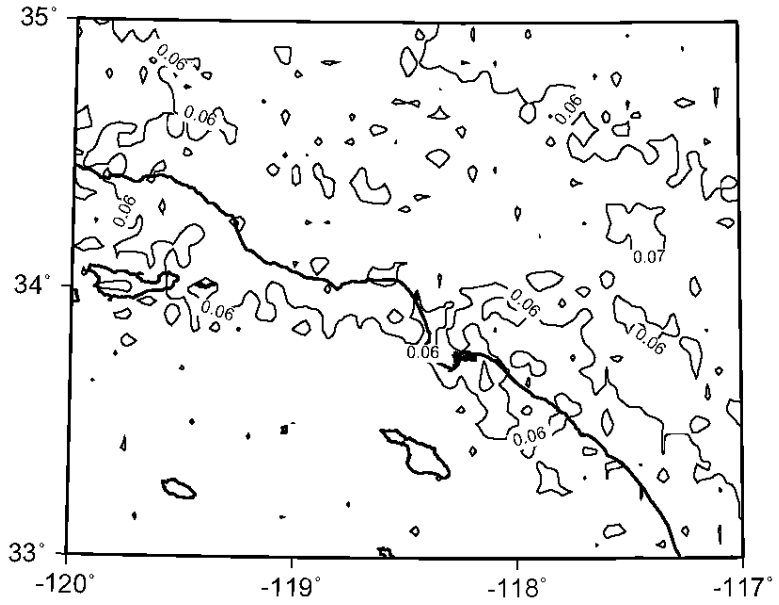

Fig. 6

Vs30 Uncertainty Only

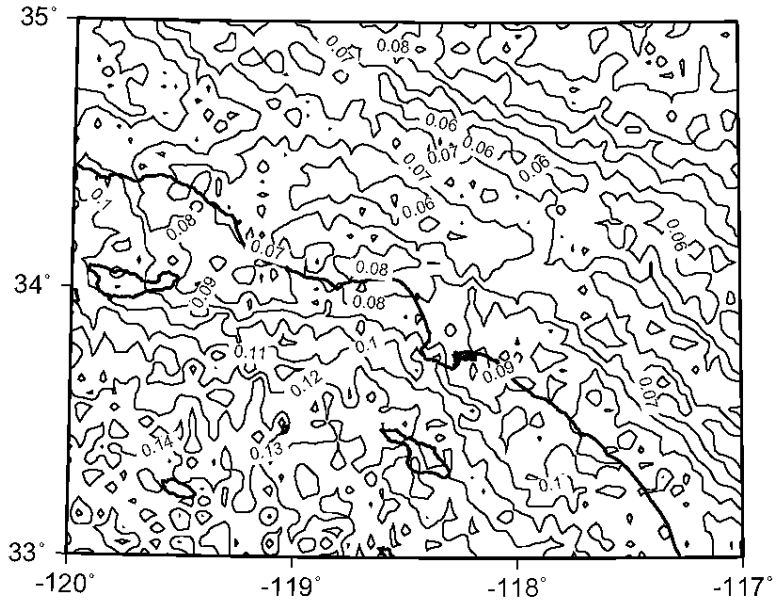

Fig. 7

All Uncertainties

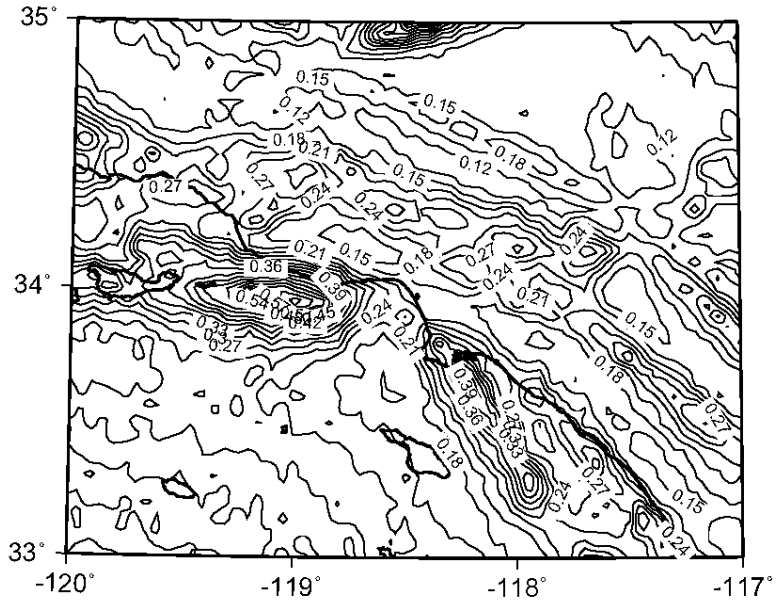

Fig. 8

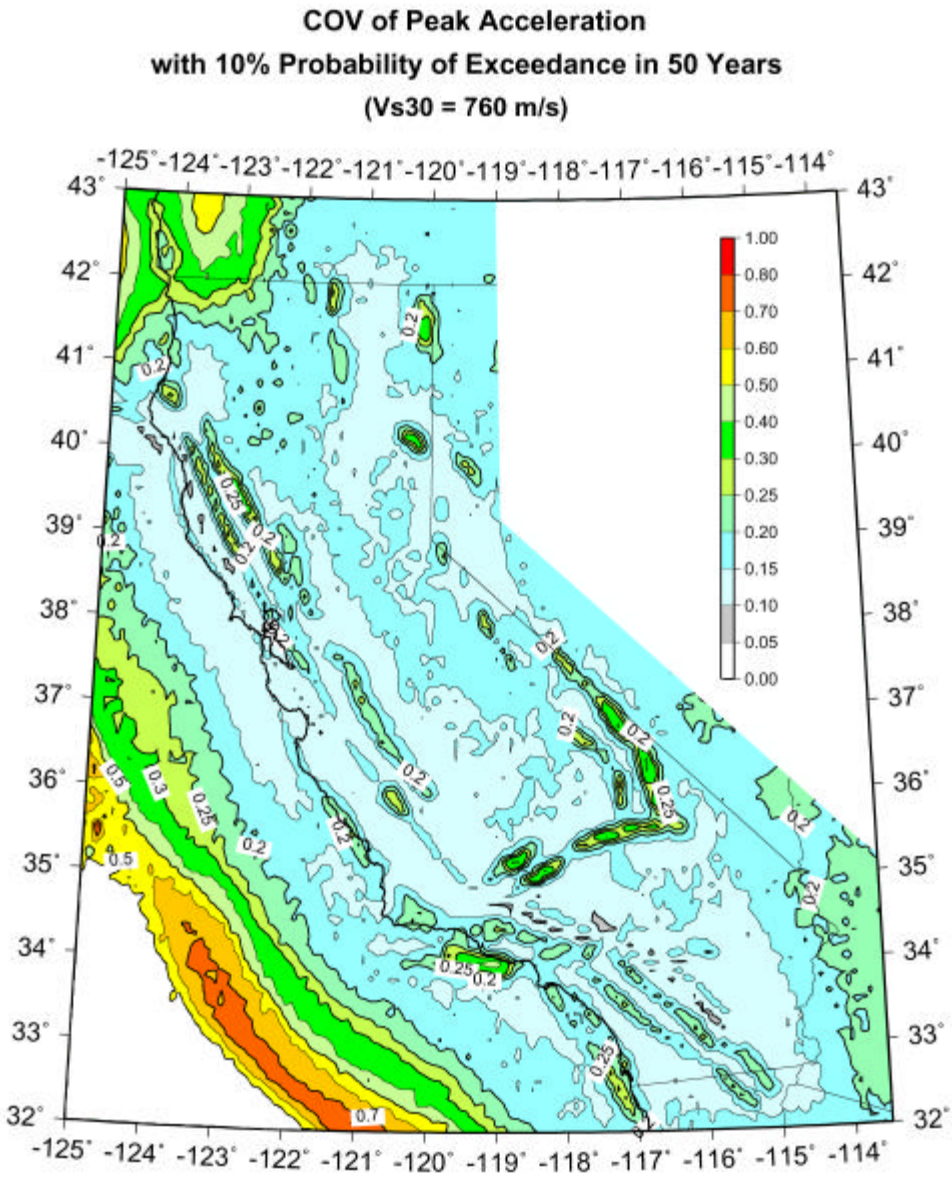
COV of Peak Acceleration
with 10% Probability of Exceedance in 50 Years
(Vs30 = 760 m/s)
-125° -124° -123° -122° -121° -120° -119° -118° -117° -116° -115° -114°
43° 42° 41° 40° 39° 38° 37° 36° 35° 34° 33° 32°
1.00
0.80
0.70
0.60
0.50
0.40
0.30
0.25
0.20
0.15
0.10
0.05
0.00

Fig. 9

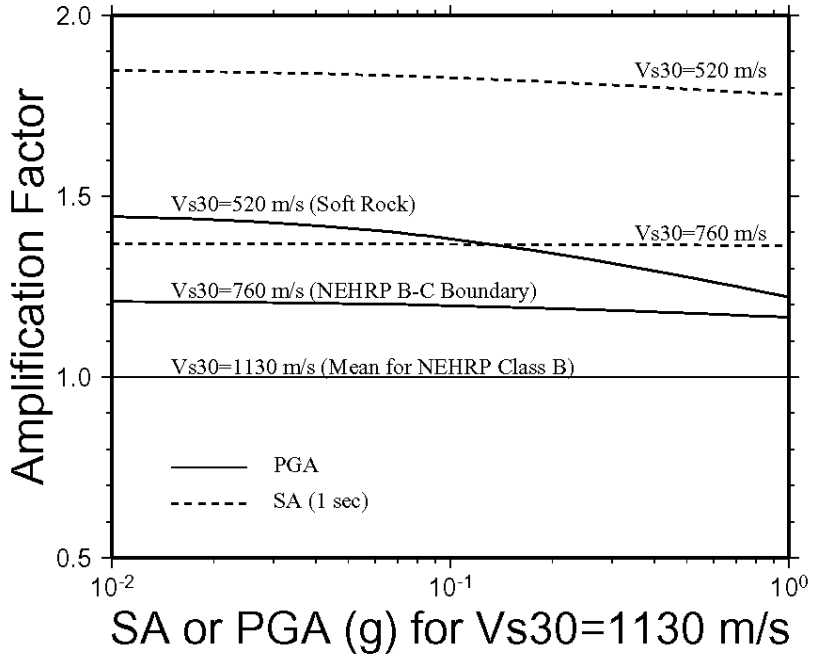
2.0
1.5
1.0
0.5
Amplification Factor
Vs30=520 m/s
Vs30=520 m/s (Soft Rock)
Vs30=760 m/s
Vs30=760 m/s (NEHRP B-C Boundary)
Vs30=1130 m/s (Mean for NEHRP Class B)
PGA
SA (1 sec)
10^{-2}
10^{-1}
10^{0}
SA or PGA (g) for Vs30=1130 m/s

Fig. 10